Soft Matter

Accepted Manuscript

ROYAL SOCIETY OF CHEMISTRY

www.rsc.org/softmatter

ARTICLE TYPE www. rsc.org/xxxxxx | XXXXXXXX

Robust liquid-infused surfaces through patterned wettability

Jason S. Wexler[a], Abigail Grosskopf[a], Melissa Chow[a], Yuyang Fan[a], Ian Jacobi[a,b], Howard A. Stone*[a]

Received Xth XXXXXXXXXX 20XX, Accepted Xth XXXXXXXXX 20XX
First published on the web Xth XXXXXXXXXX 200X
DOI: 10.1039/b000000x

Liquid-infused surfaces display advantageous properties that are normally associated with conventional gas-cushioned superhydrophobic surfaces. However, the surfaces can lose their novel properties if the infused liquid drains from the surface. We explore how drainage due to gravity or due to an external flow can be prevented through the use of chemical patterning. A small area of the overall surface is chemically treated to be preferentially wetted by the external fluid rather than the infused liquid. These sacrificial regions disrupt the continuity of the infused liquid, thereby preventing the liquid from draining from the texture. If the regions are patterned with the correct periodicity, drainage can be prevented entirely. The chemical patterns are created using spray-coating or deep-UV exposure, two facile techniques that are scalable to generate large-scale failure-resistant surfaces.

1 Introduction

Liquid-infused surfaces are micro-patterned materials that contain a thin layer of mobile liquid within their surface topography. These surfaces have received much attention in recent years due to their protective properties [1–4]. Moreover, liquid-infused surfaces have demonstrated potential as a possible alternative to traditional superhydrophobic surfaces for drag reduction [5–7]. Traditional superhydrophobic surfaces repel water and reduce drag by maintaining a thin gas layer within their surface topography. However, since the gas is compressible and soluble in the external phase, the gas layer is susceptible to pressure-induced instabilities and failure.

A major benefit of liquid-infused surfaces is that the oil that is infused into the substrate is essentially incompressible and immiscible with the external phase, and thus stable under high pressure. However, these liquid-infused surfaces are susceptible to other forms of failure. If a liquid-infused surface is oriented vertically, liquid that is initially located above the capillary rise height, L^g_∞, will drain due to gravity [8,9]. Moreover, even in the absence of gravity, liquid-infused surfaces are subject to failure due to viscous effects. We have recently shown that when a liquid-infused surface is exposed to an external, immiscible flow, the applied shear stress can drain the infused lubricating liquid [10,11].

While some of the infused liquid drains for both gravity- and shear-driven failure, a finite length of the surface remains infused indefinitely under a constant external forcing. For the shear-driven case this steady-state length is $L^s_\infty \sim f(w/h)\,\gamma/\tau$, where γ is the interfacial tension between the infused liquid and the external fluid, τ is the applied shear stress from an external flow, and w and h are characteristic dimensions of the surface texture as shown in Figure 1. This shear-driven length is analogous to the classical capillary rise height for the gravity-driven case, $L^g_\infty \sim \gamma/(\rho g w)$, with ρ as the density of the infused liquid and g as gravity.

In both cases, if the infused region of a surface is longer than the retainable length, L^g_∞ or L^s_∞, the liquid that is above or upstream of the stable region will drain. The infused liquid is retained within the stable region by a balance between the force that causes drainage, be it gravity or shear stress, and a capillary pressure gradient within the infused liquid that develops due to deformation of the fluid-fluid interface. Since the pressure gradient is inversely proportional to the wetted length, surfaces that are too long will have a pressure gradient that is too weak to counterbalance the draining force, and will drain until the wetted length reaches L^s_∞ or L^g_∞, and the capillary-induced pressure gradient becomes high enough to resist further drainage.

To create stable surfaces that are longer than L^s_∞ or L^g_∞, the texture must be interrupted by physical barriers with a period less than L^s_∞ or L^g_∞. The barriers create patches of disconnected texture that, independently, are able to resist the draining force. For applications with precisely fabricated textures, this design criterion represents a promising method for increasing the robustness of liquid-infused surfaces. However, when producing surfaces at an industrial scale, it may be prohibitively expensive to fabricate the structures needed to prevent the infused liquid from draining. Indeed, with conventional superhydrophobic surfaces, the need to produce precise micro- or nanoscale surface features that raise the threshold for pressure-driven failure has in the past been a major imped-

[a] *Department of Mechanical and Aerospace Engineering, Princeton University, Princeton, New Jersey 08544, USA. E-mail: hastone@princeton.edu*
[b] *Faculty of Aerospace Engineering, Technion – Israel Institute of Technology, Haifa 32000 Israel*

iment towards widespread implementation of these surfaces.

We propose that the infused liquid can be retained, with considerably less expense, by instead patterning regions with differing wettability on a textured surface. Surfaces with patterned wettability have been shown to be a powerful tool for manipulating droplets, rivulets, and multiphase flows[12] and thus there is reason to expect that patterned wettability on textured surfaces can be used to influence the behavior of an infused film. In an early example of patterning wettability on flat surfaces, a chemical gradient of wettability was used to move droplets against the direction of gravity[13]. Since then, advances in lithographic techniques have made it possible to create sharply defined regions of differing wettability. These sharp regions constrain static rivulets to shapes that would otherwise be unstable[14,15]; hence, stripes of preferential wettability have been used to guide rivulet flows in open microfluidic applications. For these chemically-patterned devices the flow is either imposed by a pump[16,17] or, more frequently, driven by an external force such as a surface tension gradient[18–20], an applied shear stress[21], or gravity[22,23].

In a more limited set of cases, wettability patterning has been combined with structural patterning for added functionality. For example, superhydrophobic surfaces demonstrate improved condensation performance if the top surface of the texture elements is made hydrophilic[24]. Similar patterning allows for precise control of ice nucleation[25], and in recent experiments, wettability patterning was used to control fluid invasion in liquid-infused textured surfaces[26]. In all of these cases, however, the wettability patterning has been used to add additional functionality to textured surfaces, but the idea of using such patterning to enhance the fundamental robustness of the surfaces has not been explored.

We propose that chemical patterning can be used to prevent drainage of liquid films that are infused in textured surfaces. Rather than relying on physical barriers to prevent liquid from draining under the influence of shear stress or gravity, we pattern thin stripes of a differing chemistry on the sample, separated by a distance, L, that is less than the stable capillary length, L^s_∞ or L^g_∞. The chemistry of the stripes is such that they are preferentially wetted by the external phase, be it air, water, or another fluid that is immiscible with the lubricating liquid. This chemical patterning induces the infused liquid to dewet from select regions, thereby limiting the length of continuous wetted regions to be less than the characteristic length-scale for drainage. By inducing sacrificial regions of the surface to dewet intentionally, the remainder of the surface may be made more robust. This design concept is analogous to that of a firebreak, whereby thin strips of a forest are burned intentionally in order to prevent the remainder of a forest from burning.

Patterning wettability can be accomplished through a variety of low-cost scalable techniques that are adaptable to numerous immiscible fluid systems. In this work, we demonstrate that substrates designed to be infused with either an oily liquid or an aqueous liquid can be made resistant to either shear- or gravity-driven drainage through patterned wettability. To retain infused oil against shear, we expose select regions of a hydrophobic epoxy surface to deep-UV light through a photomask, rendering these regions hydrophilic[27]. To retain an infused aqueous solution against gravitational drainage, we spray-coat select regions of a hydrophilic acrylic surface through a stencil to achieve a desired hydrophobic pattern. The treated and untreated contact angles for both surfaces are shown in Table 1, indicating that strong contrast in wettability was achieved with these techniques.

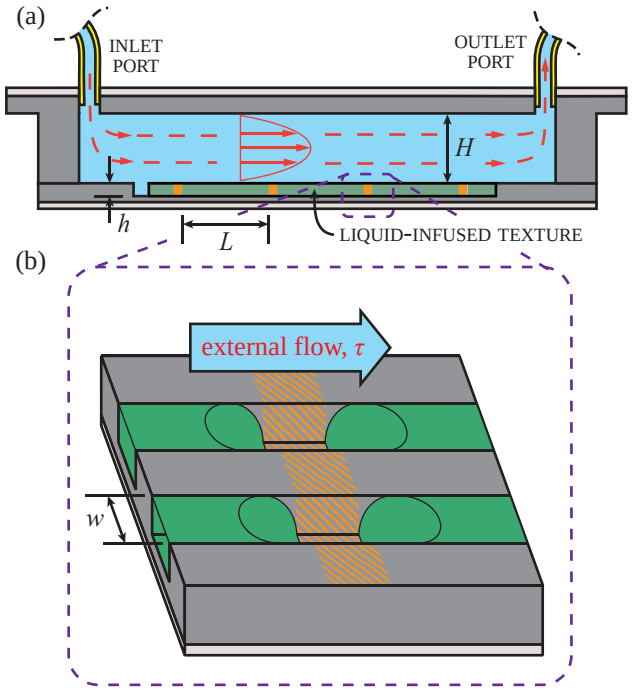

Fig. 1 (a) Schematic showing the microfluidic flow cell used to test shear-driven drainage of a liquid-infused substrate. (b) Closeup of the surface texture showing a sacrificial region. Oil is colored green and the aqueous solution is colored blue. Hydrophilic regions are denoted with orange stripes.

2 Protecting against shear-driven drainage

We start with a set of experiments to explore how patterned wettability can be used to prevent drainage of a liquid-infused substrate due to shear. A microfluidic flow cell is constructed with a texture imprinted on its floor, as in Fig. 1. This flow cell geometry is similar to that used for previous shear-driven drainage experiments[10,11]. A surface texture consisting of grooves running in the streamwise direction was chosen for the experiments, because this reduced-order geometry is con-

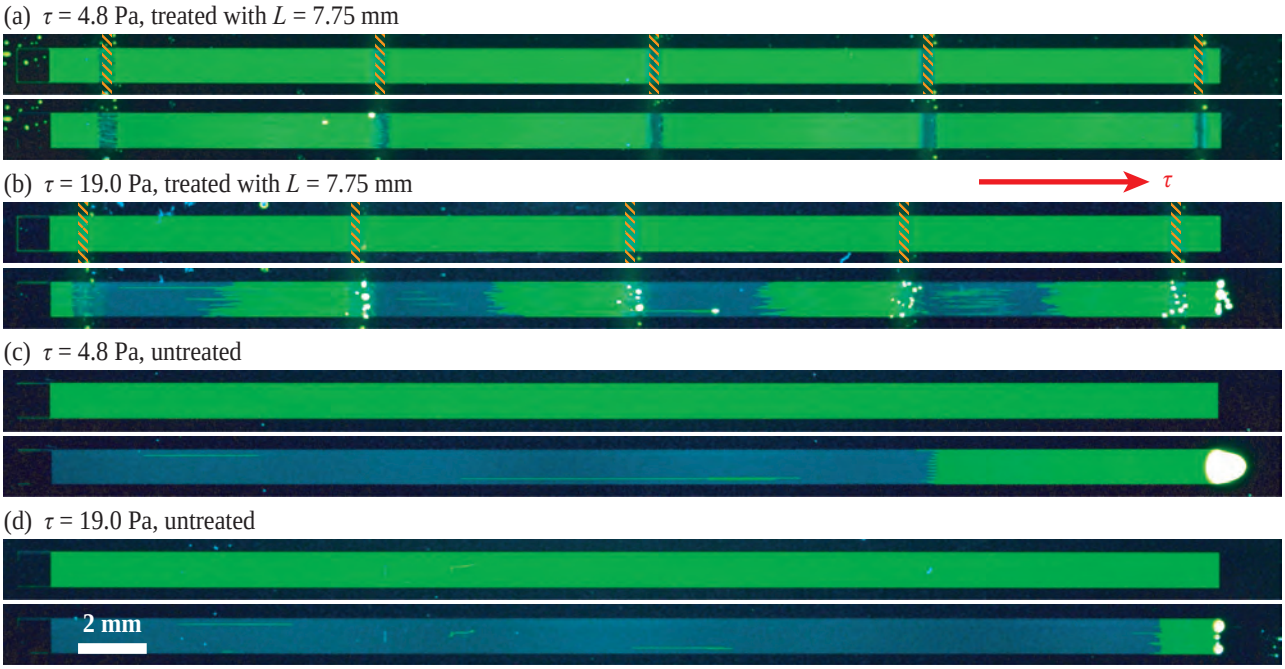

Fig. 2 Planform view of shear-driven drainage experiments conducted on surfaces with fifty streamwise grooves. Oil fluoresces green, and the drained portions of the texture reflect the blue light used for excitation. White blobs indicate the presence of overflowing oil droplets. Each image set in (a)-(d) shows the initial state (top) and the steady-state (bottom) that develops due to the designated shear stress. (a)-(b) Experiments on treated samples; hydrophilic regions are denoted in the initial state images with orange stripes. (c)-(d) Experiments on untreated samples. The scale bar in (d) applies to all images.

ducive to theoretical understanding but still captures the characteristic behavior of more complicated geometries[10].

The flow cell is constructed from Norland Optical Adhesive, a UV-cured epoxy, following the microfluidic sticker technique[28], with a depth $H = 180$ μm, a width $W = 7$ mm, and a length of 45 mm. The grooves have a width $w = 8.8 - 9.2$ μm, a depth $h = 10.0$ μm, and are 35 mm long (Fig. 1). There are fifty grooves in the texture, each separated by walls of width $11.8 - 12.2$ μm, for a total width of 1 mm. The pattern is positioned near the spanwise and streamwise center of the flow cell. Since the flow cell is very wide, with an aspect ratio of 40:1, and is much deeper than the pattern, the flow profile is approximately uniform through the width of the flow cell and parabolic through its depth. The infused liquid is silicone oil (Gelest PDM-7040, viscosity $\mu_o = 43$ mPa·s) mixed with 0.2 vol.% fluorescent dye (Tracer Products, TP-3400), and the outer aqueous liquid is a 1:1 weight mixture of glycerol and water ($\mu_{aq} = 5.2$ mPa·s). The surface tension between the two phases is $\gamma = 29$ mN/m. The outer fluid, pumped with a syringe pump at a flow rate Q, imposes a shear stress of approximately $\tau = 6\mu_{aq}Q/WH^2$ on the texture.

Norland Optical Adhesive is naturally slightly hydrophobic, so the surface must be modified in select regions to create the desired sacrificial regions of hydrophilicity. We use a method[27] that relies on deep-UV exposure to modify the surface chemistry and make the epoxy hydrophilic. The deep-UV exposure may also change the roughness of the surface, but these effects would be subsumed in the measured contact angle. The hydrophilic regions can be defined precisely through the use of a photomask. To create a photomask with micron-scale pattern geometry, a 100 nm layer of chromium is sputtered onto a bare quartz wafer; quartz is transparent in the deep-UV range. A 500 nm layer of photoresist is then spin-coated onto the quartz, before being selectively exposed and developed. After, the wafer is etched with a chromium etchant, so that unprotected regions of the chromium are dissolved. Then, the hardened photoresist is removed, leaving only the chromium photomask bonded to the quartz wafer.

The microfluidic flow cells are molded in two separate halves – an upper half with the flow cell geometry and a lower half with the grooves – before being bonded together to create a closed flow cell. Before the two sides are sealed, but after the epoxy is cured, the grooved side of the flow cell is exposed for 30 minutes under the photomask in a deep-UV lamp (Jelight bulb, intensity ≈ 30 mW/cm^2 at 253.7 nm). For the experiments presented here, the mask has transparent stripes that are 3 mm long and 250 μm wide, running across the texture with a streamwise period of 8 mm. Thus the hydrophobic

untreated regions have an approximate length of $L = 7.75$ mm as shown in Fig. 1. The mask is elevated $100 - 200$ μm above the surface of the epoxy during the patterning step, because the mask was found to damage the surface texture if it contacted the epoxy. This offset resulted in hydrophilic regions with diffuse boundaries, as well as minor variations in the geometry of the hydrophilic regions due to a non-uniform gap height. After the hydrophilic treatment the two sides of the flow cell are bonded together and the flow cells are left in an oven at 70°C overnight prior to being used.

To image the drainage dynamics over the length of the entire texture, the flow cells are mounted upside-down under a Nikon D90 camera outfitted with a 200 mm f/4 macro lens. The flow cells are illuminated with 470 nm blue LEDs that cause the oil to fluoresce. Since the fluorescence from the oil is rather weak, a number of steps are taken to enhance the image quality: a photographic filter is mounted on the lens to block the excitation light (Wratten 12 transmission spectrum), the flow cells are molded with black glass on the back side to block background light, and black fabric is wrapped around the whole setup to block light from the room.

The threshold for initial drainage can be estimated from measured properties of the substrate-fluid system though a previously derived theory that balances the external shear stress, τ, against capillary stresses (indicated by the surface tension, γ)[11]. We express the stability criterion as an inequality involving geometric and fluid properties of the substrate,

$$L < \frac{2c_p h\gamma}{c_s w\tau}\left(1+\frac{w}{2r^{\mathrm{u}}_{\mathrm{min}}}\right), \qquad (1)$$

where L is the length of continuous wetted regions. The parameters c_p and c_s are dimensionless functions of the groove aspect ratio, w/h, and $r^{\mathrm{u}}_{\mathrm{min}}$ is a length-scale that is a function of w, h, and the receding contact angle, θ_{rec} [10,11]. If inequality (1) is satisfied, the infused liquid should be stable; otherwise, it should drain.

Based on $L = 7.75$ mm in our experiments, and the other measured parameters of the system, we calculate that at a shear stress of $\tau = 12.2$ Pa the grooves should start to drain.

substrate	infused	external	θ_{adv}	θ_{rec}
epoxy	oil	aqueous	$68 \pm 1°$	$21 \pm 2°$
epoxy	oil	aqueous	$157 \pm 2°$	$55 \pm 2°$
acrylic	aqueous	air	$57 \pm 2°$	$\approx 0°$
acrylic	aqueous	air	$114 \pm 2°$	$72 \pm 2°$

Table 1 Measured wetting properties between the substrate and the infusing liquid for shear- and gravity-driven drainage experiments. Shaded rows are for the substrates that were treated to be non-wetting by the infused liquid and unshaded rows are for untreated substrates.

However, as explained previously[11], there is some amount of variability in the measured contact angles for this experimental setup, and the transitional value could be significantly lower.

At the beginning of an experiment, the entire flow cell is first filled with silicone oil. The silicone oil invades the texture, including regions that are treated to be hydrophilic, because these regions are also lipophilic in the presence of air. Then, the external aqueous solution is slowly pumped into the device at 5 μL/min, corresponding to a calculated shear stress of $\tau = 1.2 \times 10^{-3}$ Pa. The aqueous solution displaces the oil from the main portion of the channel, leaving the oil trapped in the unexposed hydrophobic regions of the texture. As the aqueous-oil interface reaches an exposed hydrophilic region, however, the aqueous solution displaces the oil from the hydrophilic region and preferentially wets this region. Thus, regions of the texture that are located between hydrophilic regions are disconnected from one another. This wetting state is shown in the top images of Fig. 2a-b, including orange stripes that indicate the exposed hydrophilic regions.

After the main portion of the flow cell has been cleared of its initial oil, the flow rate of the aqueous solution is increased rapidly to a much higher level. Experiments were performed at shear stresses of $\tau = 4.8$ and 19.0 Pa, which are below and above the estimated critical value of 12.2 Pa. Steady-state images from these two experiments are shown in Fig. 2a-b. On a surface with patterned wettability, the oil resists drainage entirely when exposed to the lower shear stress. At the higher shear stress, roughly half of each hydrophobic region is drained of oil. Control cases are shown in Fig. 2c-d, where untreated textures are exposed to the same shear stress values. In both cases, a significant portion of the texture is drained entirely of oil, indicating that our proposed method successfully prevents shear driven-drainage below a design-limited shear stress threshold, eqn (1).

A surprising feature is that the resulting wetted length in Fig. 2d is less than the individual wetted lengths in Fig. 2b. If the chemical barriers functioned exactly the same as physical barriers, we would expect these lengths to be equal. Examining the interface shape on a confocal microscope reveals that the advancing and receding contact angles in the hydrophobic regions of the treated texture are modified from those of the untreated texture, and exactly compensate for the increased wetted lengths, if these measured contact angle values are used with previously derived theories[10,11]. It is unclear why the contact angle in the unexposed region would be modified; the deep-UV treatment converts oxygen in the atmosphere to ozone, so we speculate that the ozone generated in the exposed regions diffuses into the unexposed regions and interacts with the substrate there.

Various other deep-UV treatment schemes were also tested. Experiments were performed on textures that were exposed

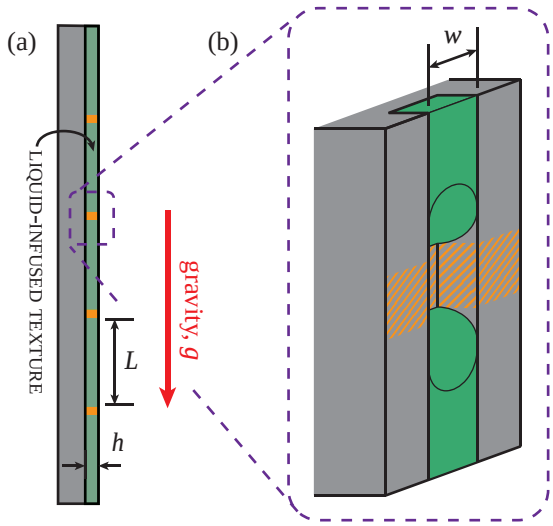

Fig. 3 (a) Schematic showing the vertical texture used to test gravity-driven drainage of a liquid-infused substrate. (b) Closeup of the surface texture showing a sacrificial hydrophobic region. Imbibed aqueous solution is colored green, and hydrophobic regions are denoted with orange stripes.

for 15 minutes and 60 minutes. The 60 minute exposure produced similar results to those shown in Fig. 2a-b, but the 15 minute exposure resulted in only partial oil retention (see Figure in Supplemental Material). The widths of the transparent stripes on the mask were also varied. When the widths were increased to 1 mm, the method worked as before. For widths of 50 μm, however, the treatment resulted in only partial oil retention, even for a 60 minute exposure time. We hypothesize that the reason for this failure is that the stripe width was significantly less than the gap between the mask and the sample, so that the UV light that reached the sample was too diffuse. This issue could potentially be resolved if a columnated light source were used instead. Alternatively, use of a photomask could be avoided entirely if a laser with a narrow beam was scanned across the sample to produce the surface treatment.

3 Protecting against gravity-driven drainage

To demonstrate the general nature of patterned wettability as a technique to retain fluids on textured surfaces, we present a second set of experiments to test gravity-driven rather than shear-driven drainage, see Fig. 3. As a further test of the retainment mechanism, we choose to design the substrate to retain an aqueous solution in the presence of air, rather than an oil in the presence of an aqueous solution. Also, an entirely different technique is utilized to achieve the contrasting chemistry: hydrophilic acrylic plastic is spray-coated through a stencil with a hydrophobic spray, resulting in regions with differing wettability. Though the drainage mechanisms, fluid systems, and surface treatments are different between these two sets of experiments, the underlying physics is analogous, and thus we expect the two sets of experiments to behave similarly.

Grooves were again used as the test geometry for the reasons stated previously, but their size was scaled up by more than an order of magnitude to demonstrate the range of length-scales at which this technique can be employed. The grooves were milled to have width $w = 0.51$ mm and depth $h = 0.51$ mm, running along the entire length of a 100 mm $\times$150 mm piece of black acrylic. The infused liquid is a 5:1 weight mixture of glycerol and water, mixed with 0.1 wt.% fluorescein sodium salt ($\rho_{aq} = 1.125$ g/mL, $\mu_{aq} = 52$ mPa·s, $\gamma = 66$ mN/m).

Carrying through the analogy with shear-driven drainage, we estimate the threshold for initial gravity-driven drainage of a liquid in a groove. Again, the stability criteria is expressed as an inequality,

$$L < \frac{2\gamma}{\rho_{aq} g w}\left(1 + \frac{w}{2r^{u}_{min}}\right), \qquad (2)$$

where L is again the length of continuous wetting regions. The parameter r^{u}_{min} is a length-scale that is a function on w, h, and θ_{rec}, as defined before[10,11]. If inequality (2) is satisfied the liquid in the groove should be stable against gravitational drainage; otherwise, it should drain.

The stability criterion in Section 2 was tested by varying the magnitude of the forcing, τ, such that eqn (1) was either satisfied or not. Rather than varying the magnitude of g (which could effectively be accomplished by adjusting the tilt-angle of the substrate), we test two different values of L that are above and below the critical value given by eqn (2). Substituting the measured parameters into eqn (2), we arrive at a threshold of $L = 46$ mm, so we test hydrophilic lengths of $L = 25$ mm and $L = 50$ mm.

To create the desired pattern of hydrophilicity and hydrophobicity, the machined acrylic was first thoroughly cleaned using isopropyl alcohol, followed by rinsing with water. The texture was then treated in an oxygen plasma chamber for 10 minutes to make it hydrophilic. To create the hydrophobic design on the texture, 1-mm thick glass microscope slides were placed over the acrylic to act as a stencil, and the glass-acrylic sandwich was spray-coated with Penguin Water & Stain Repellent. The glass microscope slides were placed such that they covered either 25-mm or 50-mm long sections of the groove, with a 2-mm exposed gap between the sections – the acrylic beneath the gap would then become hydrophobic. In order to ensure that the sprayed regions are coated uniformly, and to prevent leakage of the hydrophobic spray under the glass, the acrylic was lightly sprayed repeatedly (approximately 15 times) with 10 second intervals between each spray,

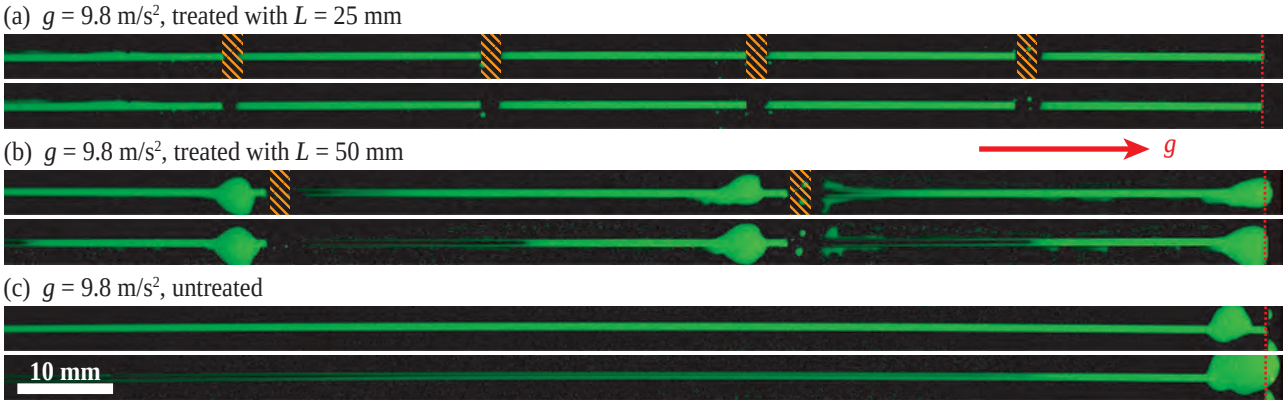

Fig. 4 Planform view from gravity-driven drainage experiments, where in this case the imbibed aqueous solution fluoresces green. The droplets at the right-most end of the images are observed to form at the end of the acrylic plate, which is marked with a dashed red line. Each image set (a)-(c) shows the configuration immediately after the plate is tilted vertically (top), and then after the system has reached a steady state (bottom). (a)-(b) Experiments on treated samples; hydrophobic regions are denoted in the initial state images with orange stripes. (c) An experiment on an untreated sample. The scale bar in (c) applies to all images.

which allowed for the spray to evaporate between repetitions and prevented pooling. The glass slides were then removed and the treated acrylic was allowed to dry in an oven at 70° C for 30 minutes.

The acrylic substrate was mounted on a stand that allowed it to be quickly rotated between a horizontal and a vertical position. While the acrylic was in the horizontal position, 1 mL of aqueous glycerol solution was distributed across one end of the texture using a syringe. The solution was then pushed along the grooves using a squeegee at approximately 20 mm/s to allow the grooves to fill with liquid. The solution only filled the hydrophilic sections of the grooves and was repelled by the hydrophobic sections. Occasionally the solution did not initially enter the hydrophilic sections, and the process was repeated until all hydrophilic sections of the grooves were filled. Drainage was initiated by quickly flipping the acrylic to the vertical position. The setup was imaged using the same macroscale fluorescent imaging as before.

Results from gravity-driven drainage experiments are shown in Fig. 4. The top images in Fig. 4a-b show the configuration for the treated substrates immediately after the acrylic is tilted vertically, with the hydrophobic regions designated using orange stripes. The hydrophilic regions in Fig. 4a have a length $L = 25$ mm, which is less than the critical value, and the hydrophilic regions in Fig. 4b have an unstable length $L = 50$ mm. Note that the groove in Fig. 4b has already started draining by the time the first image is recorded. The bottom images of 4a-b show the wetting configuration after the aqueous solution has reached a steady-state configuration. An untreated control case is included in Fig. 4c.

It is apparent that the hydrophobic stripes succeeded in preventing the infused aqueous solution from draining from the texture. The final state in Fig. 4c shows that most of the liquid has drained from the untreated groove, whereas the final state in Fig. 4a shows negligible drainage from the properly spaced regions. In Fig. 4b, which was treated to have an unstable length, L, the infused liquid has partially drained. This wetting state is very similar to the partially drained state observed in Fig. 2b, further confirming the analogy between the two sets of experiments.

4 Conclusions

Drainage from textured surfaces can be prevented by creating sacrificial regions with differing chemistry. By exploring two different drainage mechanism (shear and gravity), with two different fluid chemistries (oil/aqueous and aqueous/air), at two different length scales (10 μm and 500 μm), we have demonstrated how the sacrificial patterning technique can be broadly applied to retain liquid in a variety of liquid-infused surfaces. Both techniques for applying the surface treatment were facile and easily scalable, showing the advantage of using chemical patterning for liquid retention. In addition, a wide variety of other chemical treatment techniques potentially could be used, including conventional photolithography[26], UV-based monolayer modification[29], and laser-based processing[30]. By using this strategy of chemical patterning at length-scales comparable to the length-scale suggested by the shear- and gravity-driven drainage criteria, we have demonstrated that these two formerly limiting failure mechanisms of liquid-infused surfaces can be eliminated through minimal surface processing. Thus liquid-infused surfaces may be used in a variety of applications that were previously inaccessible, at only minimal additional expense.

5 Acknowledgements

We thank A. Kahn and G. Man for use of their deep-UV lamp, and the staff of the Princeton Micro/Nano Fabrication Laboratory for assistance with microfabrication. In addition, we thank C. Odier, R. Jeanneret, and D. Bartolo for helpful advice on implementing the microfluidic 'sticker' technique. This work was supported under ONR MURI Grants N00014-12-1-0875 and N00014-12-1-0962 (Program Manager Dr. Ki-Han Kim). We thank all team members of our MURI program for their valuable feedback.

References

1 T.-S. Wong, S. H. Kang, S. K. Y. Tang, E. J. Smythe, B. D. Hatton, A. Grinthal and J. Aizenberg, *Nature*, 2011, **477**, 443–7.
2 A. Lafuma and D. Quéré, *Europhysics Letters*, 2011, **96**, 56001.
3 A. K. Epstein, T.-S. Wong, R. A. Belisle, E. M. Boggs and J. Aizenberg, *PNAS*, 2012, **109**, 13182–7.
4 J. D. Smith, R. Dhiman, S. Anand, E. Reza-Garduno, R. Cohen, G. H. McKinley and K. K. Varanasi, *Soft Matter*, 2013, **9**, 1772–80.
5 A. Busse, N. D. Sandham, G. McHale and M. I. Newton, *Journal of Fluid Mechanics*, 2013, **727**, 488–508.
6 C. Schönecker, T. Baier and S. Hardt, *Journal of Fluid Mechanics*, 2014, **740**, 168–95.
7 B. Solomon, K. Khalil and K. Varanasi, *Langmuir*, 2014, **30**, 10970–6.
8 J. Bico, C. Tordeux and D. Quéré, *Europhysics Letters*, 2001, **55**, 214–20.
9 M. M. Weislogel, *Journal of Fluid Mechanics*, 2012, **709**, 622–47.
10 J. S. Wexler, I. Jacobi and H. A. Stone, *Physical Review Letters*, 2015, **114**, 168301.
11 I. Jacobi, J. S. Wexler and H. A. Stone, *In review*, 2015.
12 A. A. Darhuber and S. M. Troian, *Annu. Rev. Fluid Mech.*, 2005, **37**, 425–55.
13 M. Chaudhury and G. Whitesides, *Science*, 1992, **256**, 1539–41.
14 H. Gau, S. Herminghaus, P. Lenz and R. Lipowsky, *Science*, 1999, **283**, 46–9.
15 A. Pierre, M. Sadeghi, M. M. Payne, A. Facchetti, J. E. Anthony and A. C. Arias, *Advanced Materials*, 2014, **26**, 5722–5727.
16 N. Davey and A. Neild, *Journal of Colloid and Interface Science*, 2011, **357**, 534–40.
17 J. N. Tan, T. Alan and A. Neild, *AIP Advances*, 2013, **3**, 022121.
18 D. E. Kataoka and S. M. Troian, *Nature*, 1999, **402**, 794–7.
19 A. A. Darhuber, J. Z. Chen, J. M. Davis and S. M. Troian, *Philosophical Transactions of the Royal Society A*, 2004, **362**, 1037–58.
20 A. Pulido-Companys, J. Claret, J. Ignés-Mullol and F. Sagués, *Physical Review Letters*, 2013, **110**, 214506.
21 M. Rauscher, S. Dietrich and J. Koplik, *Physical Review Letters*, 2007, **98**, 224504.
22 J. Koplik, T. S. Lo, M. Rauscher and S. Dietrich, *Physics of Fluids*, 2006, **18**, 032104.
23 R. Ledesma-Aguilar, R. Nistal, A. Hernández-Machado and I. Pagonabarraga, *Nature Materials*, 2011, **10**, 367–71.
24 K. K. Varanasi, M. Hsu, N. Bhate, W. Yang and T. Deng, *Applied Physics Letters*, 2009, **95**, 094101.
25 L. Mishchenko, M. Khan, J. Aizenberg and B. D. Hatton, *Advanced Functional Materials*, 2013, **23**, 4577–4584.
26 N. Vogel, R. A. Belisle, B. Hatton, T.-S. Wong and J. Aizenberg, *Nature Communications*, 2013, **4**, 2167.
27 B. Levaché, A. Azioune, M. Bourrel, V. Studer and D. Bartolo, *Lab on a Chip*, 2012, **12**, 3028–31.
28 D. Bartolo, G. Degré, P. Nghe and V. Studer, *Lab on a Chip*, 2008, **8**, 274–9.
29 B. Zhao, J. S. Moore and D. J. Beebe, *Science*, 2001, **291**, 1023–1026.
30 H. Pazokian, A. Selimis, J. Barzin, S. Jelvani, M. Mollabashi, C. Fotakis and E. Stratakis, *Journal of Micromechanics and Microengineering*, 2012, **22**, 035001.

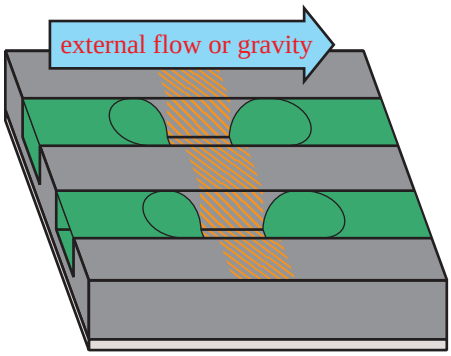

Liquid-infused surfaces can fail due to gravity, or due to shear stress from an external flow. Patterning the textured surface with regions of contrasting wettability prevents both failure modes.